

# Robust Pigtail Catheter Tip Detection in Fluoroscopy

Stratis Tzoumas, Peng Wang, Yefeng Zheng, Matthias John, Dorin Comaniciu

Siemens Corporate Research, Siemens Corporation,  
Princeton NJ, 08540, U.S.A.

**Abstract.** The pigtail catheter is a medical device inserted into the human body during interventional surgeries such as the transcatheter aortic valve implantation (TAVI). The catheter is characterized by a tightly curled end in order to remain attached to a valve pocket during the intervention, and it is used to inject contrast agent for the visualization of the vessel in fluoroscopy. Due to the different possible projection angles in fluoroscopy, the pigtail tip can appear in a variety of different shapes spanning from pure circular to ellipsoid or even line. Furthermore, the appearance of the catheter tip is radically alternated when the contrast agent is injected during the intervention or when it is occluded by other devices. All these factors make the robust real-time detection and tracking of the pigtail catheter a challenging task. To address these challenges, this paper proposes a new tree-structured, hierarchical detection scheme, based on a shape categorization of the pigtail catheter tip, and a combination of novel Haar features. Compared to previously used methods, the proposed framework offers a significant enhancement in the detection performance, providing in the same time accurate information about the orientation and the size of the detected object. The current framework has been validated on a vast data set consisting of 272 sequences, containing more than 20000 images, and the detection results demonstrate potential for clinical applications. The detection framework proposed in this disclosure is not limited to pigtail catheter detection, but it can also be applied successfully to any other shape-varying object with similar characteristics.

## 1 Introduction

During surgical interventions catheters are inserted into the patients vessels and guided to, or placed at a specific position. The automatic detection of such catheters can provide aid to the surgeon, usually in means of better visualization or motion compensation [5]. In the case of the transcatheter aortic valve implantation (TAVI) procedure, the silhouette of the extracted aorta model can be overlaid on the 2D fluoroscopic video sequence, to visually aid the physician in the placement of the artificial valve. However, the actual position of the aorta is highly influenced by a cardiac and respiratory motion, thus a mere overlay

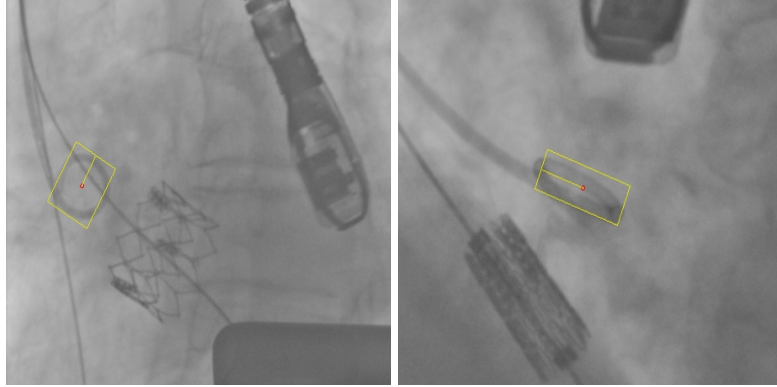


Fig. 1: Detection examples of the pigtail catheter tip.

would not be sufficient. During the TAVI intervention, an agent-injecting pigtail catheter is also inserted to the aorta. This catheter is usually inserted to a valve pocket during the intervention, following the motion of the aorta. By successfully detecting and tracking the pigtail catheter we can compensate this motion, and correctly project the 3D model of the aorta on its position in the 2D image, providing thus visualization without contrast injection.

The pigtail catheter has a tightly curled tip, the shape of which spans from pure circular to ellipsoid or even line according to the projection angle of the fluoroscopic image sequence. The appearance of the catheter tip is also radically alternated when the contrast agent is injected. Furthermore, during such interventions, a number of other devices are visible in the proximal area of the catheter causing frequent occlusion and clutter. Due to the large inter-class variation in means of shape and appearance, as well as due to the low image quality and the extended occlusion and clutter, real-time detection of the pigtail tip can be a very challenging task.

Methods traditionally used for the detection and tracking of deformable objects, as variations of Active Appearance Models [6], or a 3D model fitting approach would rely on an accurate position initialization, being thus inappropriate for this problem. Learning-based methods can provide robust, real-time results, without any prior knowledge about the position of the object. The detection framework that combines Marginal Space Learning [1] with a fast learning-based detector can promise real-time results, and it has been successfully used for the detection of medical devices in fluoroscopy [3]. The learning algorithm chosen for this particular case is the Probabilistic Boosting Tree [2], which has the ability to model and classify classes of objects with significant variation. Even this algorithm, however, faces difficulties in detecting a class of objects with very large intra-class variation using a single classifier.

In this disclosure, we propose a probabilistic framework for robust real-time detection of the pigtail catheter. The framework is based on the principles of multi-shape object detection to overcome the challenges invoked by the pigtail

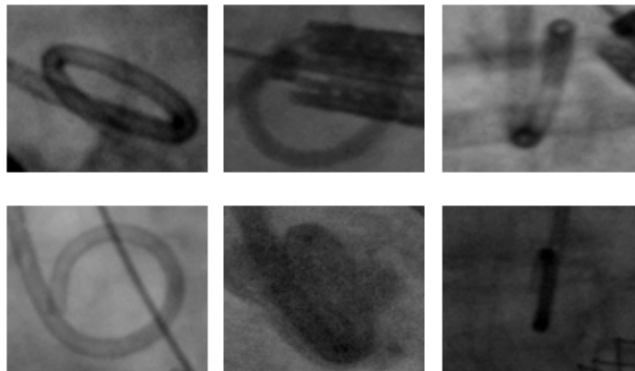


Fig. 2: Variation of the pigtail tip shape and appearance.

catheter tip shape variation. For the classification task, we use the Probabilistic Boosting Tree algorithm [2], combined with a set of Haar features [3] especially designed and selected for the pigtail case. To address the particular challenges of the pigtail object, this method makes three contributions that are organized in three individual sections in this paper:

1. In section 2, a complete shape analysis of the pigtail tip is performed and analytically presented. The object class is categorized and divided into sub-classes that appear less intra-class variation and common characteristics. The detection of each one of those sub-classes will be addressed independently according to their individuality.
2. In a second stage, a novel tree-structured detection scheme is developed to combine the sub-class detectors into a general detector for all the pigtail tip shapes. The main idea behind the proposed scheme is to reduce the complexity of the classification task as the dimensionality increases.
3. Finally, in section 4, we introduce novel Haar features that were designed and successfully used for each one of the pigtail sub-classes.

We validate this detection framework on a number of data-sets, the largest of which consists of 272 sequences (more than 20,000 images). The detection accuracy is significantly enhanced compared to previously applied methods.

## 2 A Shape Categorization of the Pigtail Catheter Tip

In an effort to simplify the detection of such a multiple-shape object, the pigtail object class is divided into three new sub-classes which have less intra-class variation, and appear common characteristics. The sub-classes created are a circular class, an ellipsoid class and a line class, and they correspond to the different angles between the projection plane of 2D fluoroscopy and the pigtail tip plane. Although it may be some ambiguous in separating the pigtail shape,

and there may be still some intra-class variation and overlap between the subclasses, this variation is significantly reduced, and can easily be handled by the property of the Probabilistic Boosting Tree algorithm of successfully modeling a rather complex distribution of a class of objects.

#### **Circular Pigtail Tip Class:**

The circular class corresponds to the majority of the cases in our data set (67%). In this case the pigtail catheter tip plane is parallel to the projection plane, so its shape appears circular in the image. The object is symmetric, corresponding to an almost rotationally independent visual appearance.

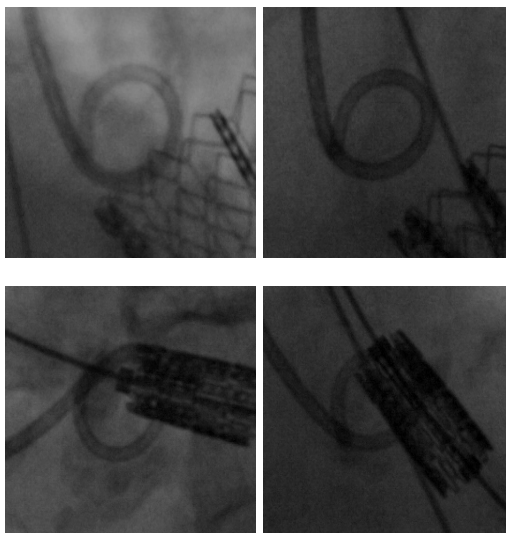


Fig. 3: Circular instances of the pigtail catheter tip

#### **Ellipsoid Pigtail Tip Class**

When the projection plane is not parallel to the catheter plane, the shape of the object appears as an ellipsoid to the image. The object is now non-symmetric, and thus its appearance is not rotationally independent. Therefore, there is a need to incorporate the orientation factor during detection. The pigtail cases categorized as ellipsoid in our data-set correspond to a percentage of 20% of the total cases.

#### **Line Pigtail Tip Class**

Finally, the pigtail catheter tip appears as a line when the projection plane is normal to the plane of the catheter tip. In this case there is also a need to search in different orientations of the image during detection. The line cases correspond to the 13% of the total cases.

Handling each one of those subclasses separately, simplifies a lot the detection procedure. A simple hierarchical detector for each one of the sub-classes

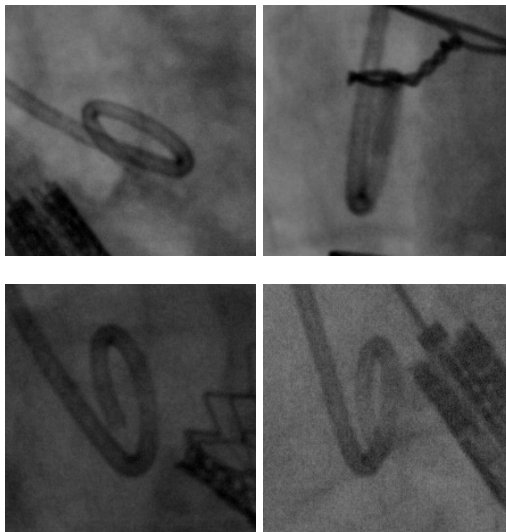


Fig. 4: Ellipsoid instances of the pigtail catheter tip

yields a significantly enhanced detection performance (6-12% enhancement in the detection rate) than the one trained for the global class. This observation suggests that the above sub-classes should be handled independently in the detection procedure, both due to their big differences in appearance and shape, as well as due to differences in primitive characteristics (e.g. symmetry).

### 3 A Tree-structured Detection Scheme for Handling Large Inter-Class Variation

For the detection of shape-varying objects, the technique that combines multiple classifiers, one for each shape of the object, has been used and proven successful in the past [4]. In this framework, this idea is combined with the principles of Marginal Space Learning in order to create a hierarchical tree-structured detection scheme that will be able to provide accurate and fast results for objects with significant shape and appearance variation, as the pigtail catheter tip.

The idea of Marginal Space Learning was introduced for the purpose of speed enhancement of detections in the 3D space [1], but it has also been successfully modified for the 2D space [3]. The idea proposes a hierarchical array of detectors, where the dimensionality of the searching space increases from the low to the higher levels in the hierarchy. The combination of this hierarchical detection scheme with an array of shape-specific detectors, yields a tree-structured detection scheme where the classification process splits as the searching space expands. When applied to shape-varying objects, this algorithm can deliver better detection rates and more accurate results, while in same time retaining high speed performance.

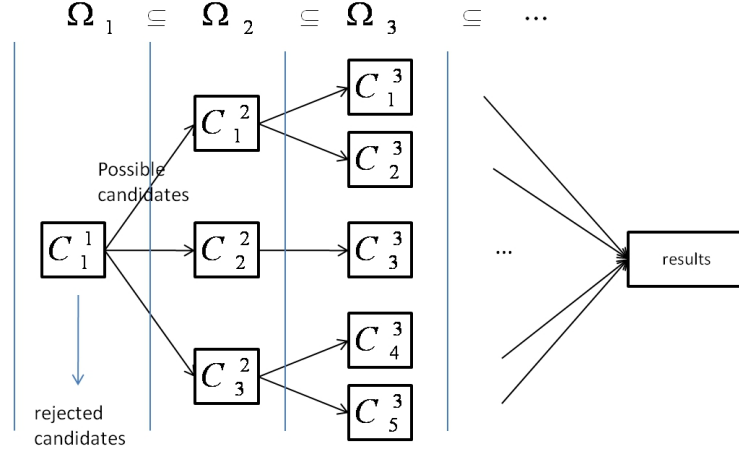


Fig. 5: Illustration of the tree-structured detection scheme.

### 3.1 Algorithm Description

Fig.5 illustrates a structural representation of this detection scheme. Let  $\Omega_1, \Omega_2, \dots, \Omega_n$  be subsets of the complete searching space with  $\Omega_1 \subseteq \Omega_2 \subseteq \dots \subseteq \Omega_n$ . Each level  $i$  of the tree corresponds to a search space  $\Omega_i$  that is a superset of the previous level searching space  $\Omega_{i-1}$  and a subset of the next level  $\Omega_{i+1}$ , as depicted in Fig. 5. The nodes  $C_i^{dim}$  of the tree represent classifiers, each of which is trained for a specific object class. The children of each node correspond to sub-classes of the parent class. Each node of the tree classifies the candidates received from its parent node, rejects a part of them, and propagates the rest as possible candidates to its children. The candidates that are propagated to the next tree level are then re-sampled according to the search space expansion before being classified. The process is probabilistic and the probability of each candidate is incrementally updated as the candidate is propagated from the root node to the leaves of the tree. In the last layer of the tree, the remaining candidates are merged and sorted according to their probability.

Let  $class_{dim,i}$  be the sub-class of objects that corresponds to the classifier in the node  $C_i^{dim}$ . Defining the operator *super* as:

$$super(class_{n,i}) = class_{n-1,k}$$

where  $class_{n,i}$  is a subclass of  $class_{n-1,k}$  we can define the following recursive type for the computation of the probability in each node  $C_i^{dim}$  of the tree:

$$P_{\Omega_{dim}}(Z, class_{dim,k}) = P_{\Omega_{dim}}(Z|class_{dim,k})P_{\Omega_{dim-1}}(Z, super(class_{dim,k})) \quad (1)$$

Where  $P_{\Omega_{dim-1}}(Z, super(class_{dim,k}))$  is the prior probability attributed to the candidate from the previous nodes, and  $P_{\Omega_{dim}}(Z|class_{dim,k})$  is the probability

according to the classification in node  $C_i^{dim}$ . With the above recursive type defining the probability of the leaves, we can compute the posterior probability of each input candidate  $Z$  by the following equation:

$$P_{post}(Z) = \|P_{\Omega_N}(Z, class_{N,1}), P_{\Omega_N}(Z, class_{N,2}), \dots, P_{\Omega_N}(Z, class_{N,K})\|_{\infty} \quad (2)$$

Where  $K$  is the number of leaves of the tree (number of classes in the last layer) and  $N$  is the depth of the tree (number of divisions in the search space).

### 3.2 Application to the pigtail catheter tip

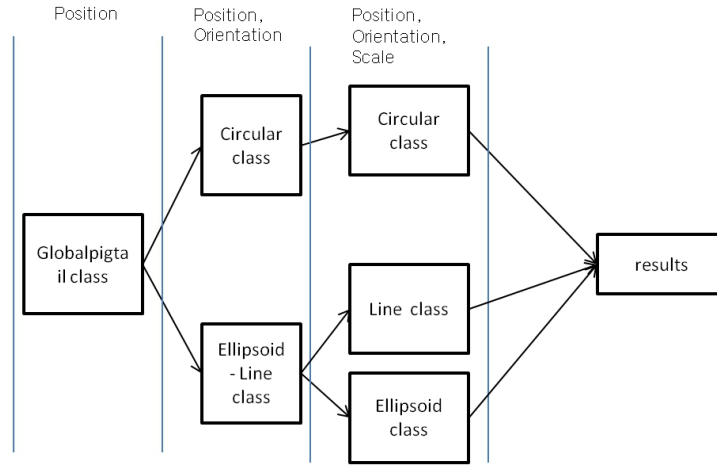


Fig. 6: Illustration of tree detection structure for the pigtail case.

For the pigtail case, the tree detection scheme described above is used and combined with the pigtail catheter tip shape categorization that has been described in Section 2. Every node of the tree corresponds to a hierarchical classifier trained with the Probabilistic Boosting Tree algorithm for a specific sub-class of the data set. The root of the tree corresponds to a global classifier for all the pigtail shapes. This classifier searches only for the position in the space, performing early non-object areas rejection. The purpose of the root classifier is to feed most of the possible objects as candidates to the next level of the tree, while rejecting most of the non-object regions. In the following levels of the tree, the different object sub-classes are handled independently as depicted in Fig. 6:

For the circular case a hierarchical detector, that has been trained only with circular pigtail instances, is applied to the candidates. This detector samples the candidates in different orientations but since the circular case is approximately symmetric, this sampling can be rather sparse. For the ellipsoid and line cases, a single hierarchical detector is applied to the candidates. The orientation sampling

needs to be significantly denser in this case. The ellipsoid and line cases are handled together for speed enhancement and because they correspond to small sub-sets of our dataset. However there can be a further discrimination in the last stage of the hierarchy for more accurate results.

In the end, the detection results from all leaf nodes are merged, and the best detections are selected as an output.

#### 4 Circular Haar features

Haar features have been widely used in many types of object detection due to their computational efficiency and their ability to capture primitive information of the image. For the purposes of pigtail tip detection we use an extended set of 14 Haar features especially designed for medical devices [3]. Furthermore, we introduce a novel Haar feature that has the ability to capture the circular shape of the pigtail catheter tip. By handling independently the detection of circular and ellipsoid instances of the pigtail tip, we are able to use different features in each case, according to the specificities of the corresponding shape.

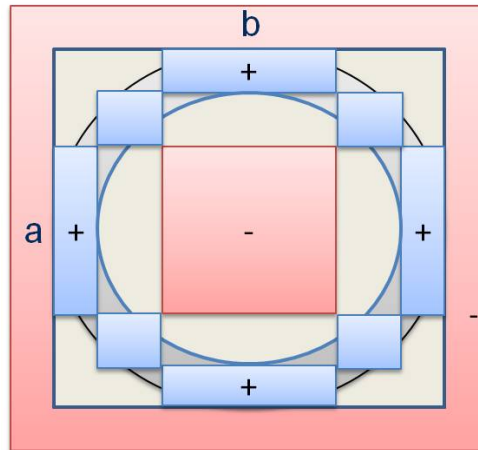


Fig. 7: Circular Haar feature.

For the circular instances of the pigtail catheter, a complex Haar feature has been designed in order to capture the circular shape. This novel circular feature is visualized in Fig. 7. The positive area of the feature is the one represented with blue color, and the negative is the one with the red color in the figure. The negative area consists of an inside and an outside part, that are normalized so that they will contribute the same to the final summation. The bandwidth of the positive areas, and the lengths  $a$  and  $b$  constitute configurable parameters, which are optimized for the case of the Pigtail after simulations on the circular

and ellipsoid shape. More specifically, the parameters  $a$  and  $b$  are proportional to the height and width of the feature according to the equations  $a = width/f_1$  and  $b = height/f_2$ . The dividing factors  $f_1$  and  $f_2$  range from 2.25 to 3 according to whether the shape of the feature is pure circular or ellipsoid. According to our experiment, the new feature appears to be very dominant and successful for the circular case, as it is selected very often, and usually first, by the AdaBoost algorithm.

For the modelling of the ellipsoid instances of the pigtail tip, the two-directional features described in [3] appear to be particularly successful and most often selected by the AdaBoost algorithm. The two-directional features quantify the relationship of conventional Haar features at two orthogonal directions, capturing in this way the horizontal or vertical deployment of the object.

## 5 Experiments

The detection framework proposed in this disclosure, is evaluated on two datasets. The first data-set consists of 197 fluoroscopic sequences of circular and ellipsoid pigtail shapes, including partial occlusion and contrast injection. In total the first data-set consists of more than 14,000 images. The second data-set is an expansion of the first one, where a number of fully occluded cases and line instances of the pigtail tip are added. It is a more challenging data-set, and it consists of more than 20,000 images.

Data Set	Detection rate
Circular:	93.2 %
Ellipsoid:	87.9 %
Circular+Ellipsoid:	83.6 %

Table 1: Comparison between the detection performance in subsets and in the whole data-set 1

Table 1 presents the detection performance on the training set, within the sub-classes of data-set 1, and in the whole class using a single classifier for each case. There is an obvious decrease in the detection performance when the sub-classes are handled together, which confirms our assumptions in Section 2.

Table 2 provides a comparison between the hierarchical structure of single detectors for all shapes, and the tree detection strategy described in Section 3, for both data-sets. When using the tree-structured detection scheme there is an obvious enhancement in the detection rate, which rises as the data-set becomes more complex. To evaluate the generalization ability in each case, we performed 4 folder cross-validation by randomly splitting the data-set in 4 parts. The results of the cross-validation experiment suggest that the proposed detection scheme is much more robust, offering better generalization for unknown data-sets.

Data Set	Hierarchical Structure	Tree Structure
Data-Set 1: Training set	83.6 %	86.5 %
Data-Set 2: Training set	74.9 %	82.6 %
Data-Set 1: Cross Validation	76.7 %	80.3 %
Data-Set 2: Cross Validation	65.5 %	77.8 %

Table 2: Comparison between hierarchical and tree-structured detection scheme

Fig. 8 presents the detection rates on both data-sets, when taking into account the best  $n$  detections of the framework, where  $1 \leq n \leq 10$ . For the first data-set, the tree-structured framework is very successful achieving more than 86% accuracy in the first detection, and more than 97% within one of the first 10 detections. This suggests that the framework is capable of successfully detecting the pigtail tip without any prior knowledge or position initialization, and if combined with an appropriate tracking method it could yield very good tracking results, appropriate for medical applications.

The proposed framework introduces a speed overhead to the detection procedure that can be tuned however according to the speed requirements, by increasing the rejection between layers. The configuration used for the above experiments yields a speed of around 1 frame per second on 1024x1024 images searching on all possible orientations with step  $10^\circ$ , on an 8 core machine with 2GHz CPUs.

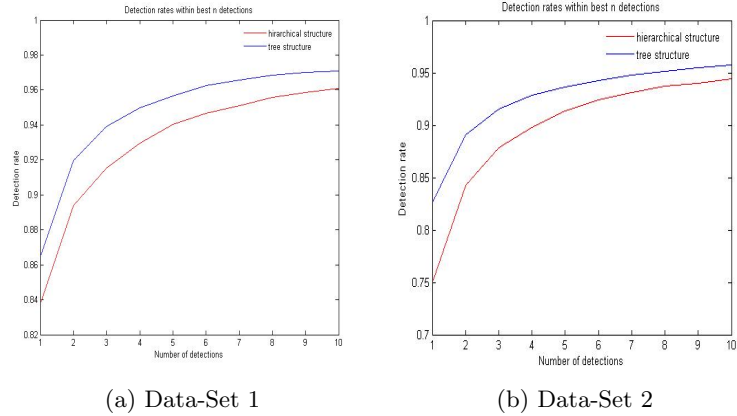


Fig. 8: Detection results.

Finally, Table 3 presents a qualitative evaluation of the detection results in data set 1. The scaling error in each direction is computed by the type:  $Error = (size(annotation) - size(detection))/size(annotation)$

Data Set	Average angle error	Average scaling error X	Average scaling error Y
Data-Set 1:	$7.7^\circ$	0.06	0.19

Table 3: Qualitative evaluation of the detection results

## 6 Conclusion

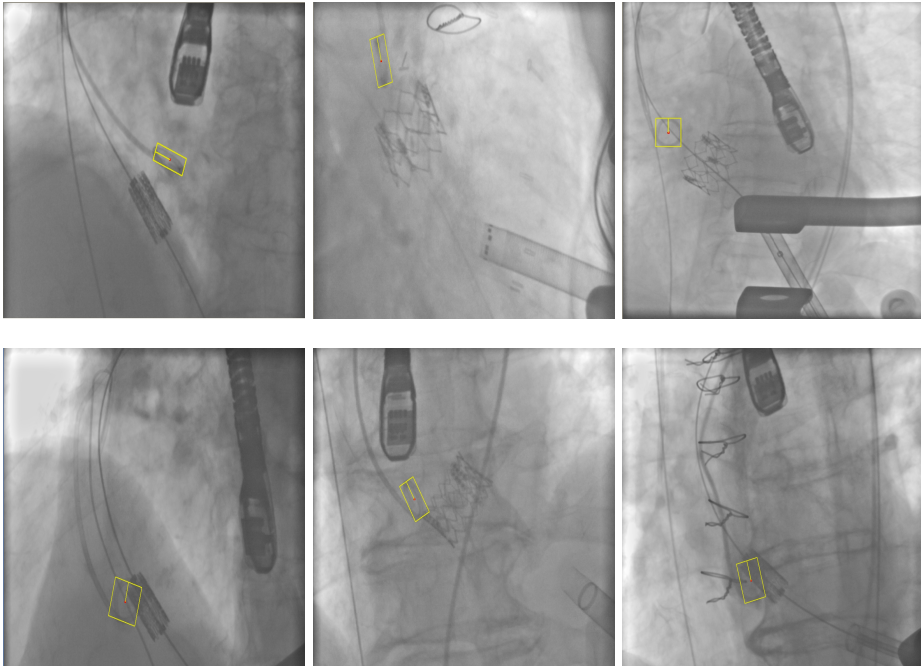


Fig. 9: Visual Illustration of correct detection results

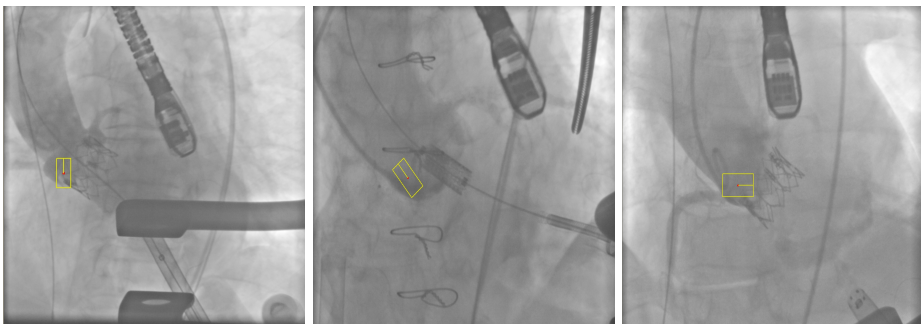


Fig. 10: Visual Illustration of false detection results

In this disclosure, we propose a learning-based detection framework for the localization of the pigtail catheter tip in fluoroscopic video sequences. For the classification task we use the Probabilistic Boosting Tree algorithm, for its capability to model classes of objects with large inter-class variation, and an extended set of Haar-like features. To address the challenges invoked by the shape variation of the object, we propose a tree-structured detection scheme that is based on the principles of Marginal Space Learning. The above framework is capable of providing accurate detection results, in terms of position, orientation and scale, it is robust to occlusion and it applies globally to all possible shape deformations of the pigtail tip.

## References

1. Yefeng Zheng; Barbu, A.; Georgescu, B.; Scheuering, M.; Comaniciu, D.; , "Fast Automatic Heart Chamber Segmentation from 3D CT Data Using Marginal Space Learning and Steerable Features," Computer Vision, 2007. ICCV 2007. IEEE 11th International Conference on , vol., no., pp.1-8, 14-21 Oct. 2007
2. Zhuowen Tu; , "Probabilistic boosting-tree: learning discriminative models for classification, recognition, and clustering," Computer Vision, 2005. ICCV 2005. Tenth IEEE International Conference on , vol.2, no., pp.1589-1596 Vol. 2, 17-21 Oct. 2005
3. Peng Wang, Terrence Chen, Shaohua Zhou, Dorin Comaniciu, Martin Ostermeier, The Design of Features and Detector for the Device Detection and Tracking in Fluoroscopy, U.S. Intervention Disclosure 2010E19150US
4. Peng Wang, Qiang Ji, "Multi-View Face Detection under Complex Scene based on Combined SVMs," Pattern Recognition, International Conference on, pp. 179-182, 17th International Conference on Pattern Recognition (ICPR'04) - Volume 4, 2004
5. Peng Wang; Marcus, P.; Chen, T.; Comaniciu, D.; , "Using needle detection and tracking for motion compensation in abdominal interventions," Biomedical Imaging: From Nano to Macro, 2010 IEEE International Symposium on , vol., no., pp.612-615, 14-17 April 2010
6. T.F. Cootes, G. J. Edwards, and C. J. Taylor. Active appearance models. ECCV, 2:484498, 1998